Heslop, J. K., Anthony, K. M. W., Grosse, G., Liebner, S., Winkel, M. (2019): Century-scale time since permafrost thaw affects temperature sensitivity of net methane production in thermokarst-lake and talik sediments. - *Science of the Total Environment*, *691*, pp. 124—134.

DOI: http://doi.org/10.1016/j.scitotenv.2019.06.402

Title

Century-scale time since permafrost thaw affects temperature sensitivity of net methane production in thermokarst-lake and talik sediments

Authors

J. K. Heslop[1*], K. M. Walter Anthony[1], G. Grosse[2,3], S. Liebner[4,5], M. Winkel[1,4]

Affiliations

[1]Water and Environmental Research Center, University of Alaska, Fairbanks, USA

[2]Alfred Wegener Institute Helmholtz Centre for Polar and Marine Research, Potsdam, Germany

[3]Institute of Earth and Environmental Sciences, University of Potsdam, Germany

[4]GFZ German Research Centre for Geosciences Hemholtz Centre Potsdam, Postdam, Germany

[5]Institute of Biochemistry and Biology, University of Potsdam, Germany

[*]Present address: Department of Geography and Planning, Queen's University, Kingston, Canada

Corresponding author

J. Heslop, Department of Geography and Planning, Mackintosh-Corry Hall, Rm D102A, Queen's University, Kingston ON K7L 3N6, 343-333-9925 (phone), 613-533-6122 (fax), joannekheslop@gmail.com (email)

Abstract

Permafrost thaw subjects previously frozen soil organic carbon (SOC) to microbial degradation to the greenhouse gases carbon dioxide (CO_2) and methane (CH_4). Emission of these gases constitutes a positive feedback to climate warming. Among numerous uncertainties in estimating the strength of this permafrost carbon feedback (PCF), two are: (i) how mineralization of permafrost SOC thawed in saturated anaerobic conditions responds to changes in temperature and (ii) how microbial communities and temperature sensitivities change over time since thaw. To address these uncertainties, we utilized a thermokarst-lake sediment core as a natural chronosequence where SOC thawed and incubated *in situ* under saturated anaerobic conditions for up to 400 years following permafrost thaw. Initial microbial communities were characterized, and sediments were anaerobically incubated in the lab at four temperatures (0 °C, 3 °C, 10 °C, and 25 °C) bracketing those observed in the lake's talik. Net CH_4 production in freshly-thawed sediments near the downward-expanding thaw boundary at the base of the talik were most sensitive to warming at the lower incubation temperatures (0 °C to 3 °C), while the overlying sediments which had been thawed for centuries had initial low abundant methanogenic communities (< 0.02%) and did not experience statistically significant increases in net CH_4 production potentials until higher incubation temperatures (10 °C to 25 °C). We propose these observed differences in temperature sensitivities are due to differences in SOM quality and functional microbial community composition that evolve over time; however further research is necessary to better constrain the roles of these factors in determining temperature controls on anaerobic C mineralization.

Keywords

carbon, lake sediments, methane, permafrost, talik, temperature sensitivity

41 **Graphical Abstract**

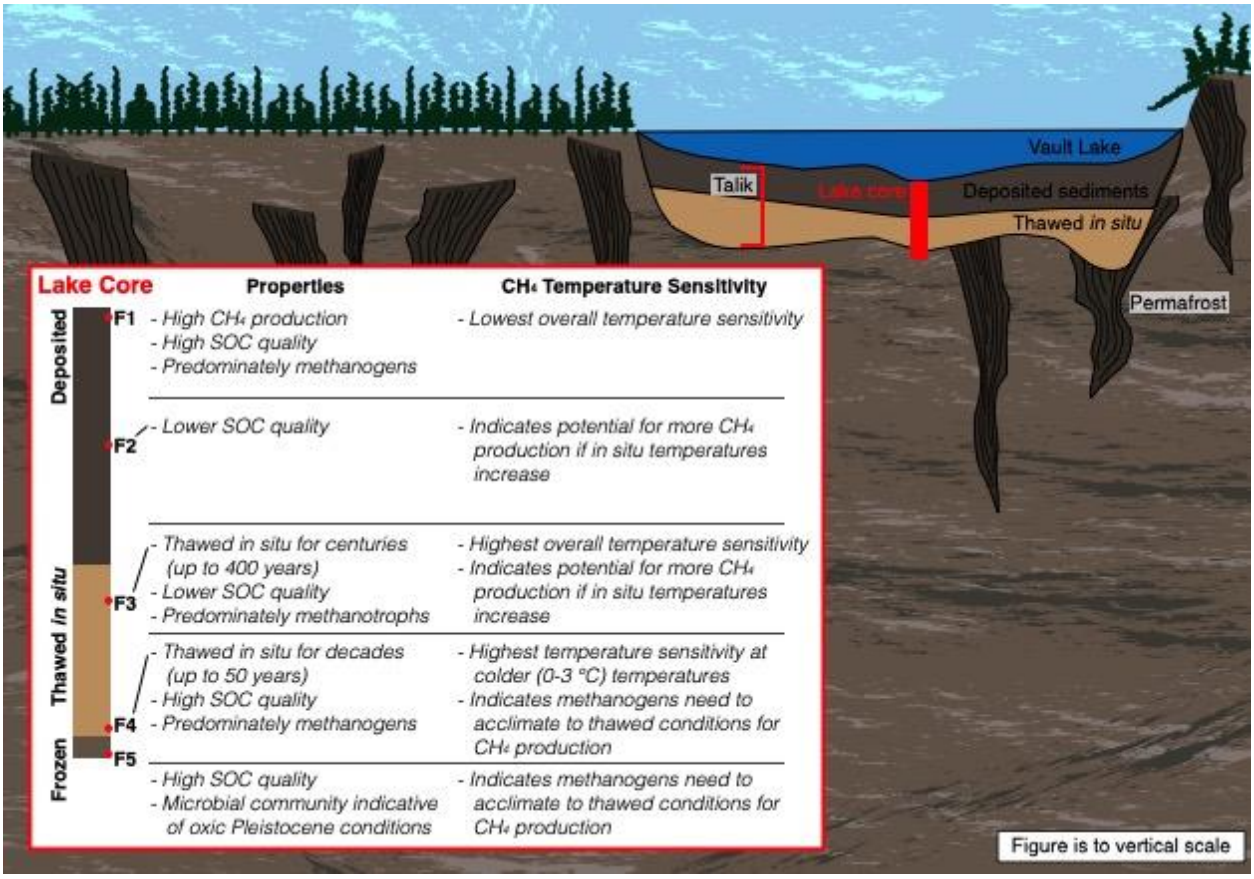

42

Highlights

- Time since permafrost thaw affects microbe communities and temperature sensitivity
- Recently-thawed sediments had highest temperature sensitivities at low temperatures
- Sediment thawed for centuries was most sensitive to warming at high temperatures
- Deposited sediment produced the most CH_4 but had the lowest temperature sensitivity

Abbreviations

BH	borehole
C	carbon
CH_4	methane
CO_2	carbon dioxide
F	facies
OM	organic matter
OTU	operational taxonomic units
PCF	permafrost carbon feedback
PCR	polymerase chain reaction
R	ratios of C-CH_4 production potentials
SOC	soil organic carbon
SOM	soil organic matter

1. Introduction

Permafrost landscapes contain an estimated 1,330-1,580 Pg of soil organic carbon (SOC), representing about one-third of total global SOC stocks (Hugelius et al., 2014, Schuur et al., 2015). Defined as ground at or below 0 °C for at least two consecutive years, permafrost covers about 24% of land surface in the Northern Hemisphere (Zhang et al., 1999). Air temperature records suggest high latitudes (>60 °N) are warming twice as fast as the remainder of the globe (Bekryaev et al., 2010, Schuur et al., 2015), and climate models predict amplified Arctic warming will continue into the coming century. Globally, permafrost temperatures have increased by an average of 0.29 °C during the past decade (Biskaborn et al., 2019). Permafrost warming and subsequent thaw lead to the mobilization and potential microbial degradation of previously frozen, inactive permafrost SOC (Davidson and Janssens, 2006, Olefeldt et al., 2013, Schuur et al., 2015, Yang et al., 2016). Microbial degradation converts permafrost SOC into the greenhouse gases carbon dioxide (CO_2) and methane (CH_4), which, when released to the atmosphere, cause a positive feedback to climate warming known as the permafrost carbon feedback (PCF; Walter et al., 2006, Schuur et al., 2015).

Permafrost thaw also changes local and regional hydrology, leading to fragmented wetting and drying of the landscape (Jorgenson et al., 2013). Landscape wetting and drying play an important role in controlling whether thawed SOC will be mineralized aerobically as CO_2 or anaerobically as CO_2 and CH_4. While it has been suggested that permafrost SOC mineralization in aerobic conditions releases an average of 3.4 times more C ($C\text{-}CO_2$) than SOC mineralization in anaerobic conditions ($C\text{-}CO_2$ + $C\text{-}CO_2$; Schädel et al., 2016), CH_4 emissions from permafrost environments are expected to become more important over longer time scales (beyond 2100; Dean et al., 2018). CH_4 production rates in saturated, anaerobic systems are more sensitive to

variability in soil temperature than C mineralization in drier, aerobic ecosystems (Olefeldt et al., 2013, Schädel et al., 2016). A recent synthesis of 21 aerobic and anaerobic permafrost soil incubation studies found that a 10 °C increase in temperature (5 °C to 15 °C) resulted in net C release increasing by a factor of 2.0 (i.e. mean Q_{10} = 2.0, 95% CI = 1.8-2.2; Schädel et al., 2016). However, ranges of previously reported temperature sensitivity values vary between permafrost SOC mineralized under aerobic versus anaerobic conditions. In permafrost soils, previously observed anaerobic C mineralization ($C\text{-}CO_2$ + $C\text{-}CH_4$) Q_{10} values ranged from 1.2 to 22.0 (Čapek et al., 2015, Chowdhury et al., 2015, Treat et al., 2015, Schädel et al., 2016) while, in aerobic conditions, Q_{10} values for $C\text{-}CO_2$ ranged from 1.6 to 9.4 (Mikan et al., 2002, Čapek et al., 2015, Bracho et al., 2016, Schädel et al., 2016). Given that CH_4 has a 34 times higher global warming potential than CO_2 over a century time scale (Myhre et al., 2013), and that northern soils are expected to warm during the next several decades and beyond (Guo and Wang, 2016), it is important to understand CH_4 production responses to temperature increases to fully estimate the potential strength of the PCF.

SOC mobilization and mineralization from thawing permafrost are expected to become a long-term C source, projected to contribute accelerating rates of C emissions over the coming centuries (10 Pg C by 2100, 50 Pg C by 2200, 120 Pg C by 2300; Parazoo et al., 2018). Therefore, in addition to requiring a better understanding of how CH_4 production changes with temperature, modeling the potential PCF will require better estimates of how temperature sensitivities change over century-scale time since permafrost thaw. It is difficult to obtain this information from incubations and field warming experiments, which commonly capture temperature responses of labile SOC fractions with fast (days to years) turnover times (Conant et al., 2011, Bracho et al., 2016, Knoblauch et al., 2013, 2018). In permafrost soils, the size of this

fast C pool is small (< 5%) and the majority (> 95%) of permafrost SOC has turnover times of decades to centuries (Schädel et al., 2014). Temperature sensitivities of these slower C pools are largely unknown (Conant et al., 2011).

Natural chronosequences, where SOC has incubated *in situ*, provide unique opportunities to examine how temperature sensitivity of SOC mineralization changes over time. Due to their formation and thaw histories, thermokarst lake taliks (thaw bulbs) can provide a unique natural laboratory in which permafrost SOC has thawed and incubated *in situ* under saturated anaerobic conditions for hundreds to thousands of years (West and Plug, 2008, Kessler et al, 2012). Thermokarst lakes are known to have high rates of CH_4 emission (Sepulveda-Jauregui et al., 2014, Walter Anthony et al., 2018), with the organic matter (OM) substrate for methanogenesis primarily originating from permafrost SOC thawing both beneath and surrounding the lake (Kling and Kipphut, 1991, Zimov et al., 1997, Walter et al., 2008, Brosius et al., 2012, Walter Anthony and Anthony, 2013, Lenz et al., 2016). In surface lake sediments, decomposition of deposited contemporary OM fuels methanogenesis (Walter Anthony et al., 2014, Elder et al., 2018). Once formed, thermokarst lakes strongly alter the local ground thermal balance by transferring heat from the water body to the underlying ground more effectively than other land cover types (Burn, 2005, Grosse et al., 2012, Jorgenson et al., 2013), which can subsequently trigger downward permafrost thaw and talik formation beneath the lake (Plug and West, 2009). After accounting for initial SOC heterogeneity in the vertical profile, the thawed permafrost soils beneath a thermokarst lake represent a natural chronosequence of time since thaw, with sediments closest to the thaw boundary at the base of the talik being the most recently thawed.

Here, we anaerobically incubated sediments from a thermokarst lake core with the objective of examining the temperature sensitivity of CH_4 production. We examined how both *in*

131 *situ* microbial communities and temperature sensitivities of net CH_4 production change over
132 century time scales since permafrost thaw. Our work involved monitoring temperature along two
133 vertical profiles in the thermokarst lake talik, characterizing *in situ* microbial communities at
134 different depths within the talik, incubating sediments at four temperatures bracketing those
135 found within the talik, and calculating temperature sensitivities of net CH_4 production at different
136 depths within the talik and at different incubation temperature intervals. We show how microbial
137 community composition and temperature sensitivity of net CH_4 production potentials change
138 with depth, using depth as a proxy for increasing time since thaw in the talik. While microbial
139 communities have been characterized in near-surface (<1.5 m) thermokarst-lake sediments (He et
140 al., 2012, Negandhi et al., 2013, Crevecoeur et al., 2016, Matheus Carnevali et al., 2018), to our
141 knowledge this is the first study to examine changes in initial microbial communities at deeper
142 depths (up to 5.9 m) in a thermokarst-lake talik and along a centuries-scale time-since-thaw
143 chronosequence. We also compare microbial community composition and net CH_4 production
144 temperature sensitivity between surface sediments deposited by erosion from the surrounding
145 environment with the underlying thawed *in situ* permafrost.
146
147 **2. Materials and methods**
148 *2.1. Vault Lake sediment core description*
149 During March 2013, a 590-cm long sediment core was collected from the center of Vault
150 Lake, Alaska, USA (65.0293 ºN, 147.6987 ºW) using methods described in detail in Heslop et al.
151 (2015). Based on ^{14}C-dating of macrofossils picked from the sediment core, Vault Lake was
152 estimated to have formed ca. 400 cal. years BP (Heslop et al., 2015). Heslop et al. (2015)
153 classified and described in detail the lake profile subdivided into five sediment facies: (F-1)

surface organic-rich mud, (F-2) lacustrine silt, (F-3) taberite, (F-4) recently-thawed taberite, and (F-5) frozen transitional permafrost. Briefly, the surface organic-rich mud facies (F-1, 0-152 cm) represents organic-rich sediments deposited following lake formation, which were exposed to the lake water column and settled to the lake bottom. The lacustrine silt (F-2, 153-330 cm) facies represents material that sloughed off the thermokarst lake margin and was exposed to the lake water column during erosion and re-deposition. The lowest three facies (F-3, F-4, F-5, >330 cm) comprise the taberite sequence, consisting of Pleistocene-aged yedoma permafrost that either thawed *in situ* or is presently thawing and transitioning to taberite beneath the lake. Yedoma refers to permafrost formed due to syngenetic sediment, peat, and ice accumulation in unglaciated regions during the Pleistocene and contains high ice and OC contents compared to other mineral-type permafrost soils (Zimov et al., 2006, Strauss et al., 2017). The taberite facies (F-3, 331-507 cm) represents yedoma sediments which thawed *in situ* beneath the lake during the past ~400 years since lake formation; the bottom section of the taberite, which we estimate thawed within the past ~50 years based on talik growth functions of Kessler et al. (2012), was designated as the recently-thawed taberite facies (F-4, 508-550 cm). The frozen portion of the core beneath the talik that is currently thawing and transitioning to taberite was designated as the transitional permafrost facies (F-5, 551-590 cm). Taberite sediments are silt-rich, but lack aquatic macrofossils since they thawed beneath the lake without contacting the overlying water column. Multivariate statistical analyses conducted by Heslop et al. (2017) on geochemical and sediment OM molecular composition data from the core indicate sediments from the surface organic-rich mud facies contained different SOM characteristic than the bottom four facies (F-2 lacustrine silt, F-3 taberite, F-4 recently-thawed taberite, and F-5 frozen transitional permafrost), which contained statistically homogenous SOM. Due to the statistical homogeneity of their SOM

(Heslop et al., 2017) and their history of thawing *in situ* beneath Vault Lake, we interpret the three lower facies (F-3, F-4, F-5) to represent a 400-year chronosequence of time since permafrost thaw.

2.2. Vertical temperature profile measurements

Temperature below the sediment-water interface at Vault Lake was measured in galvanized steel tubes placed in two boreholes [Borehole (BH) 10 and BH13] described in Heslop et al. (2015). At BH10, located 6.1 m from an actively expanding thermokarst margin in 2013 (Figure 1), the talik thickness was 8.6 m and the lake water column was 1.4 m depth. At BH13, located in the center of the lake, farther away from the expanding margins, the lake water column was deeper (4.0 m) and the talik was thinner (5.7 m). At each borehole, we installed temperature sensors (Onset TMCx-HD, accuracy ± 0.21˚C) at four depths below the sediment-water interface and recorded temperatures hourly from May 2013-April 2019. The temperature sensor depths were representative of the F-1 surface organic-rich mud (BH10 and BH13: 0.5 m and 1.0 m), the F-3 taberite (BH10: 6.2 m), the F-4 recently-thawed taberite (BH13: 5.7 m), and the F-5 frozen transitional permafrost (BH10: 8.9 m, BH13: 6.2 m) facies.

2.3. Anaerobic sediment incubations

We prepared and incubated sediment slurries [mean ± SD 262 ± 121 g dw sediment L^{-1}; range 124-455 g dw sediment L^{-1}] from five depths in the core, representing one depth from each of the five facies described above (Table 1), using methods previously described in Heslop et al. (2015). Briefly, we used a stir bar to homogenize 150 ±70 cc of lake core sediment with 750 mL O_2-free, sterilized DI water (Milli-Q) while purging the slurry with ultra-high-purity (UHP) N_2 gas (Air Liquide). Fifty mL of the homogenized slurry were transferred to each 100 mL glass serum incubation vial, and each vial was flushed with a constant stream of UHP N_2 gas for 5

minutes prior to being sealed with butyl rubber stoppers and aluminum crimp caps. L-cysteine (Sigma-Aldrich) was injected in each vial to a concentration of 0.025% wt/v to serve as a reducing agent, and anaerobic conditions were verified by measuring initial headspace O_2 concentrations using gas chromatography (Shimadzu GC-2014). For each core depth, we incubated sediment slurries in triplicate at four temperatures (0 °C, 3 °C, 10 °C, and 25 °C) bracketing those found within thermokarst-lake environments. Incubation temperatures were selected to be representative of temperatures measured in the Vault Lake talik using methods described above (0 °C, 3 °C, 10 °C) and previously published upper bounds for permafrost OC incubation studies (25 °C; Vonk et al., 2015). We measured headspace CH_4, N_2, and O_2 concentration monthly using gas chromatography (Shimadzu GC-2014; detection limits 0.1 ppm, 50 ppm, and 50 ppm for CH_4, N_2, and O_2, respectively) for a period totaling 150 days. Cumulative C-CH_4 production potential (mg C-CH_4) was calculated as the total mass of net C-CH_4 produced in each incubation vial during the 150-d incubation period normalized by the mass of initial SOC in each bottle (mg C-CH_4 g SOC^{-1}).

2.4. Temperature sensitivity calculations

We calculate temperature sensitivity in our incubations using two methods. We first calculate temperature sensitivity across all our incubation temperatures as the slope of a linear regression between the log of cumulative net C-CH_4 production (mg C-CH_4 g SOC^{-1}) and incubation temperature (°C; Gudasz et al., 2015). For each facies, cumulative net C-CH_4 production of each incubation vial at each incubation temperature was treated as one observation (n = 1) in the linear regression. Because we treat each incubation vial as one observation, we use the GC CH_4 detection limit (0.1 ppm CH_4,) to calculate potential analytical error in measured C-CH_4 production. Linear regressions were calculated for each facie (n = 12 observations per facie)

223 using MATLAB R2016a software, and 95% confidence intervals were calculated for the slope
224 and intersect in each linear regression. We report the slope (temperature sensitivity) of the
225 regression line for each facies, the p-value of the calculated slope, and the R^2 value of the
226 calculated slope fit to the observations (Table S1, Figure 2).

227 To differentiate between temperature sensitivities at colder versus warmer incubation
228 temperatures for each facies, we also calculated ratios of the mean cumulative net C-CH_4
229 production potentials from the triplicate incubation vials for pairs of incubation temperature
230 treatments (3 °C : 0 °C ; 10 °C : 0 °C; 25 °C : 0 °C; 10 °C : 3 °C; 25 °C : 10 °C). Temperature
231 sensitivities were calculated as ratios, as opposed to using Q_{10} values, to account for variables
232 such as functional microbial community size and composition that diverge with temperature
233 during long-term incubations (Bracho et al., 2016) and subsequently affect CH_4 production rates
234 (Wagner et al., 2007, Knoblauch et al., 2013, 2018), potentially causing misrepresentative Q_{10}
235 values for net CH_4 production.

236 *2.5. Microbial community analysis*

237 We characterized the microbial community composition at four of our incubation facies
238 (F-1 surface-rich organic mud and the taberite sequence F-3, F-4, and F-5) using sediment
239 collected adjacent to the incubated sediments from the same lake core. Given the analyzed
240 sediment subsamples were collected adjacent to the incubated sediment subsamples, we assumed
241 measured microbial communities are representative of microbial communities both *in situ* and at
242 the start of our incubations. Sediments were collected using a sterilized spatula, placed in a
243 sterilized glass vial, sealed, and immediately frozen until further analyses. Genomic DNA of 4.7-
244 13 g sediment was extracted using the protocol of Zhou et al. (1996). DNA concentrations were

quantified with a Nanophotometer® P360 (Implen GmbH) and Qubit® 2.0 Flurometer (Thermo Fisher Scientific).

The 16S rRNA gene for bacteria was amplified with the primer combination S-D-Bact-0341-a-S-17 and S-D-Bact-0785-a-A-21 (Herlemann et al., 2011). The 16S rRNA gene for archaea was amplified in a nested approach with the primer combination S-D-Arch-0020-a-S-19 and S-D-Arch-0958-a-A-19 in the first polymerase chain reaction (PCR) for 40 cycles and S-D-Arch-0349-a-S-17 and S-D-Arch-0786-a-A-20 in the second PCR for 35 cycles, respectively. The primers were labelled with unique combinations of barcodes. The PCR mix contained 1x PCR buffer (Tris•Cl, KCl, $(NH_4)2SO_4$, 15 mM $MgCl_2$; pH 8.7; QIAGEN), 0.5 µM of each primer (Biomers), 0.2 mM of each deoxynucleoside (Thermo Fisher Scientific), and 0.025U μl^{-1} hot start polymerase (QIAGEN). The thermocycler conditions were: 95°C for 5 min (denaturation), followed by 40 cycles of 95°C for 1 min (denaturation), 56°C for 45 seconds (annealing) and 72°C for 1 minute and 30 sec (elongation), and concluding with a final elongation step at 72°C for 10 min. PCR products were purified with a Hi Yield® Gel/PCR DNA fragment extraction kit (Süd-Laborbedarf). PCR products of three individual runs per sample were combined. PCR products of different samples were pooled in equimolar concentrations and compressed to a final volume 10 µl with a concentration of 200ng μl^{-1} in a vacuum centrifuge Concentrator Plus (Eppendorf). Individual samples were sequenced in duplicates. Illumina sequencing was performed by GATC Biotech AG using 300 bp paired-end mode. Due to different sequencing length, we used 20% PhiX control v3 library for better performance.

The quality of the sequences was checked using the fastqc tool (http://www.bioinformatics.babraham.ac.uk/projects/fastqc/ by S. Andrews). Sequence raw reads

were demultiplexed and barcodes were removed with the CutAdapt tool (trim-n; e 0.1; only consider exact barcodes for mapping; Martin, 2011). The subsequent steps included merging of reads using overlapping sequence regions PEAR (Q 25; p 0.0001; v 20; Zhang et al., 2014), standardizing the nucleotide sequence orientation, and trimming and filtering of low quality sequences using Trimmomatic (SE; LEADING Q25; TRAILING Q25; SLIDINGWINDOW 5:25; MINLEN 200; Bolger et al., 2014). After quality filtering, chimera were removed by the ChimeraSlayer tool of the QIIME pipeline. Subsequently, sequences were clustered into operational taxonomic units (OTU) at a nucleotide cutoff level of 97% similarity and singeltons were automatically deleted. To reduce noise in the dataset, sequences with relative abundances below 0.1% per sample were also removed. All archaeal libraries contained at least 14,300 sequences, while bacterial libraries contained at least >71,400 sequences. OTUs were taxonomically assigned employing the Silva database release 128 (Quast et al., 2012) using the QIIME pipeline (Caporaso et al., 2010). Older taxonomic assignments for archaea and bacteria were manually corrected according to new publications, e.g. Micellaneous Crenarchaeal Group (MCG) was renamed to *Bathyarchaeota* (Rinke et al., 2013, Castelle et al., 2015, Adam et al., 2017).

Sequences have been deposited at NCBI under the Bioproject PRJNA381521with the sequence read archive accession numbers SRX3047223- SRX3047228 for bacterial and SRX3047230- SRX3047235 for archaeal sequences, respectively.

2.6. Statistics

All statistical analyses were conducted using MATLAB R2016a software. Values from each triplicate incubation vial were treated as n=1 for all statistical analyses. We determined if CH_4 production potentials significantly deferred between facies (selected facie versus remaining

facies at the same incubation temperature) and with warming incubation temperatures (colder v. warmer temperature for the same facies) using two-sample t-tests. We considered differences between facies and incubation temperatures statistically significant when $p \leq 0.05$.

3. Results

3.1. Temperatures in the Vault Lake talik

Temperature data were recorded continuously, except for a data gap between 25 July and 11 November 2014; a period between 18-20 January 2017, during which very cold atmospheric temperatures interfered with the logger operation; and 24 October 2017 to 7 April 2018 in BH13, due to an animal chewing through wiring. In the profile adjacent to the southern thermokarst margin (BH10) hourly temperatures recorded from May 2013 to October 2017 ranged from -0.40 to 14.45 ˚C (annual mean ± SD 2.50 ± 3.37 ˚C; Figure 1). In the center of Vault Lake (BH13), observed temperatures in the vertical profile ranged from -0.40 to 4.51 ˚C (annual mean ± SD 1.11 ± 1.42 ˚C; Figure 1). In both profiles, the shallow sediment depths (50-100 cm below the sediment-water interface) were warmer (0.14 to 14.45 ˚C) and showed clear seasonal variations compared to the deepest (5.70 m and 8.85 m) sediments near the thaw boundary (-0.40 to 2.37 ˚C), which showed less seasonal variation. Mean annual temperature was 3.26 ± 2.94 ˚C in the shallower sediments and 0.18 ± 0.59 ˚C near the thaw boundary.

3.2. Net CH_4 production potentials

Net CH_4 production potentials roughly increased with increasing incubation temperatures (Figures 2, S2) in all samples except the F-5 frozen transitional permafrost samples, in which the net CH_4 production potential was highest at the 3 ˚C incubation temperature. Cumulative net C-CH_4 production potentials during the 150-d incubation ranged from 0.0 to 610 mg C-CH_4 g SOC^-

^{1} (Figures 2, S2). Except for at the 25 ˚C incubation temperature, the F-1 surface organic-rich mud facies produced the most net C-CH_4. At the 25 ˚C incubation temperature, the F-3 taberite facies produced the most net C-CH_4 g SOC^{-1} (610 mg C-CH_4 g SOC^{-1}). The F-5 frozen transitional permafrost produced the least net C-CH_4 at all incubation temperatures except at 3 ˚C. At the 3 ˚C incubation temperature, the F-3 taberite facies produced the least net C-CH_4 g SOC^{-1}. Full net C-CH_4 production potential results are presented in Figures 2 and S2.

3.3. Temperature sensitivities

Temperature sensitivities at each facies, calculated across all incubation temperatures, ranged from 0.11 to 0.42 (Table S1, Figure 2). The F-1 organic-rich mud facies had the lowest overall temperature sensitivity, while the F-3 taberite facies had the highest overall temperature sensitivity. Ratios (R) of net C-CH_4 production potentials between different incubation temperatures in our study ranged from 0.01 to 99,200 (Table 2). At the coldest temperature interval (3 ºC : 0 ºC), the F-4 recently-thawed taberite and the F-5 frozen transitional permafrost had the highest R values. At the remaining temperature intervals, the F-3 taberite facies had the highest R values in our study. Full R results are presented in Table 2.

3.4. Microbial community composition

The initial archaeal communities of the F-1 mud and F-4 recently-thawed taberite facies were dominated by methanogens such as *Methanobacteriaceae, Methanoregulaceae, Methanosaetaceae*, and *Methanosarcinaceae*, which collectively accounted for ~84% to 89% of all sequences. The F-3 taberite facies exclusively revealed *Methanoperedenaceae* sequences belonging to the anaerobic methanotrophic clade ANME-2d (Winkel et al., 2019). *Methanoperedenaceae*/ANME-2d were also detected in F-4 (1%) and F-5 (15%) facies. In addition to methanogens and anaerobic methanotrophs, facies F-5 contained high relative

sequence abundances of *Bathyarchaeota* (24%), metabolic generalists widespread in anaerobic systems, and ammonia-oxidizing *Thaumarchaeota*/ *Nitrososphaerales* (21%; Figure 3).

The initial bacterial communities in all facies were dominated by *Actinobacteria, Chloroflexi, Firmicutes, Alphaproteobacteria,* and *Betaproteobacteria*, which collectively contributed 71-85% of all bacterial sequences. Certain taxa only appeared in high relative abundances in specific facies of the Vault lake core (Figure 4). Taxa such as *Plantomycetes* and *Saccharibacteria* only appeared in the F-4 recently-thawed taberite, *Gemmatimonadetes* appeared only in the F-3 and F-4 facies, and *Gammaproteobacteria* was only observed in the F-1 organic-rich mud.

4. Discussion

Short-time scale studies (days to years) have shown that time is an important factor in determining temperature sensitivity of C mineralization, but how temperature sensitivity changes over long (decades to centuries) time scales is poorly understood. Understanding changes in temperature sensitivity over these longer time scales is vital to improve estimates of the long-term magnitude of the PCF. Our study utilizes a unique approach for examining how potential net CH_4 production changes in the decades to centuries following permafrost thaw under saturated anaerobic conditions. Our results suggest that net CH_4 production in sediments at the base of the talik (decadal time scales since thaw) are most sensitive to temperature increases at lower temperatures, while net CH_4 production in sediments which have been thawed for longer periods of time (centuries time scales) were most sensitive at higher temperatures (Table 2). We attribute these changes to differences in available substrate and microbial community acclimation.

4.1. Temperature sensitivities at decadal timescales since thaw

The F-5 transitional permafrost facies immediately below the thaw boundary had lower CH_4 production potential values and lower temperature sensitivity (overall temperature sensitivity and 0 °C to 3 °C R values) than the F-4 recently-thawed taberite immediately above the thaw boundary. We acknowledge that slopes used to calculate overall temperature sensitivities at the F-4 and F-5 facies had lower ($R^2 < 0.33$) fit to our data compared to the slopes of the overlying (F-1, F-2, and F-3) facies, and p-values which were significant at the $\alpha = 0.10$ level but not at the $\alpha = 0.05$ level. The lower R^2 values in the F-4 and F-5 facies are influenced by the significant increases in CH_4 production between 0 °C to 3 °C at these facies, which we discuss below. Sediments from the F-5 transitional permafrost facies were frozen when the sediment core was collected and thawed at the commencement of the incubation, and we estimate sediments in the F-4 recently-thawed taberite thawed within the past 50 years (Heslop et al., 2015). This result is consistent with findings from anaerobic incubations of sediment cores from ice wedge polygons collected in Northern Alaska, where soils above the thaw boundary produced more CH_4 and had greater temperature sensitivity of CH_4 production than soils from the underlying permafrost (Zheng et al., 2018).

We observed the highest 0 °C to 3 °C R values in the F-4 recently-thawed taberite and F-5 transitional permafrost facies. The 0 °C to 3 °C temperature interval is representative of temperature increases as permafrost thaws and warms and is consistent with *in situ* temperatures observed in the temperature profiles at the base of the talik below Vault Lake (BH13 5.7 m and 6.2 m depth; BH10 8.9 m depth). We postulate the high net CH_4 temperature sensitivity values observed in these facies at this temperature interval are due to a combination of a rapid increase in CH_4-producing communities following thaw and freshly-thawed sediments containing greater

proportions of fresher, more labile SOC compared to the overlying sediments thawed for longer periods of time.

Methanogens are known to be naturally present in permafrost environments (this study; Rivinka et al., 2000, Mackelprang et al., 2017, Malard and Pearce, 2018). While methanogenic activity has been measured at temperatures as low as -20 °C (Rivinka et al., 2000), CH_4 production rates in permafrost are extremely low due to a lack of activation energy to initiate the chemical reactions involved in CH_4 production (Davidson and Janssens, 2006, Conant et al., 2011). Permafrost warming and thaw have been associated with increases in the number of methanogens and subsequent CH_4 production rates (Knoblauch et al., 2018, Wei et al., 2018). We suggest an initial, rapid bloom in methanogen biomass following thaw and the subsequent mineralization of accumulated, biolabile permafrost SOC compounds due to the input of heat energy may contribute to the high 0 °C to 3 °C R values we observed in the F-4 and F-5 facies. Microbial community composition has also been found to control C decomposition responses to changes in temperature and precipitation in temperate aerobic systems (Glassman et al., 2018).

Archaeal communities in the F-4 recently-thawed taberite facies were dominated (89% relative abundance) by methanogens and contained low initial abundance (1%) of methanotrophs (Figure 5). The archaeal community in the F-4 facies mainly revealed acetoclastic methanogens of the family *Methanosaetaceae* (64%), which are known to be specialist for cold neutral environments (Wen et al., 2017). The initial microbial communities in the F-4 facies also showed sequences related to bacteria (*Firmicutes-Clostridiales, Betaproteobacteria-Rhodocyclales,* and *Actinobacteria*) that are known as soil fermenters in low temperature soil and can produce precursors for methanogens such as acetate, formate and H_2 (Tveit et al., 2015). In comparison, the observed taxa *Saccharibacteria, Burkholderiales, Actionmycetales*, and *Bathyarchaeota* in

406 the F-5 transitional permafrost facies are suggestive of the presence of organic material that
407 needs to break down from polymers to fermentation products, which in turn can be used as
408 substrate for methanogens. The microbial community in the F-5 facies also showed many taxa
409 (*Alphaproteobacteria-Caulobacterales/Rhizobiales/Rhodospiralles*, *Planctomycetes-Pirellulales*,
410 and *Thaumarchaeota-Nitrososphaerales*) that are indicative for oxic conditions during
411 permafrost formation in the Pleistocene. These results suggest changes in microbial community
412 composition and biomass during decadal time scales following thaw, which we propose
413 contribute to the increases we observed in net CH_4 production potentials at the 0 °C to 3 °C
414 temperature interval near the thaw boundary.
415 In thermokarst lake environments, the permafrost thaw boundary at the outer extent of the
416 lake's talik has been previously identified as a region of high CH_4 production (Kessler et al.,
417 2012, Walter Anthony et al., 2016). We propose this is due to the CH_4-producing microbial
418 communities observed in the F-4 facies consuming recently-thawed, previously unavailable
419 permafrost OM. In both thermokarst and non-thermokarst lake sediments, CH_4 production has
420 been shown to be highly dependent on substrate availability (Gudasz et al., 2015, de Jong et al.,
421 2018) Permafrost warming and thaw near the thaw boundary remove a major physical barrier to
422 C mineralization, initializing the rapid mineralization of the most biolabile SOM compounds
423 (Davidson and Janssens, 2006, Drake et al, 2015, Yang et al., 2016). Independent analyses of
424 frozen permafrost from the Vault Creek site revealed high proportions of reduced, low molecular
425 weight compounds in the water-extractable fraction of the SOC (Heslop et al., 2019). These
426 compounds are considered highly bioavailable and are rapidly depleted following permafrost
427 thaw (Spencer et al., 2015, Drake et al., 2015, 2018).

Our results suggest there is an initial spike in net CH_4 production in the decades following permafrost thaw under anaerobic conditions. We attribute this to CH_4-producing microbial communities, which may not have been active in the frozen permafrost, acclimating to thawed conditions, stabilizing, and consuming accumulated bioavailable SOC. Our results suggest net CH_4 production in freshly-thawed sediments will increase as methanogen communities acclimate to thawed conditions. These results are consistent with a recent study which suggested, following establishment of stable CH_4-producing microbial communities, equal amounts of CO_2 and CH_4 were produced from thawing permafrost SOC (Knoblauch et al., 2018).

4.2. Temperature sensitivities at century timescales since thaw

Our results suggest that the initial increase in net CH_4 production at current *in situ* temperatures during decadal time scales since permafrost thaw (F-4 and F-5) will not be sustained over century time scales following thaw (F-3). This is consistent with findings from long-term field temperature sensitivity studies conducted in aerobic, non-permafrost systems, which suggest initial increases in SOC mineralization upon the first several years of warming do not persist (Conant et al., 2011). Compared to the underlying F-4 recently-thawed taberite facies, the F-3 taberite facies, representing permafrost which has been thawed for longer periods of time (up to 400 years based on estimated lake age; Heslop et al., 2015), had lower CH_4 production potential values at lower incubation temperatures (0 °C and 3 °C). However, at our higher incubation temperatures (10 °C and 25 °C) sediments in the F-3 facies had greater net CH_4 production and temperature sensitivity. This is consistent with examinations of boreal lake sediments, which found that increasing temperature sensitivity was coupled with decreasing C respiration (Gudasz et al., 2015). In our study, we posit the shift from net CH_4 production in recently-thawed sediments (F-4 and F-5) having the highest temperature sensitivities at colder

451 incubation temperatures to net CH_4 production in sediments which have been thawed for longer
452 periods of time (F-3) only responding to warming at higher incubation temperatures is due to
453 changes in SOC quality and *in situ* microbial community composition over century timescales.
454 SOM is composed of a continuum of compounds with increasing molecular complexity
455 and, consequently, increasing activation energies required for microbial decomposition
456 (Davidson and Janssens, 2006, Conant et al., 2011, Schädel et al., 2014, Bracho et al., 2016).
457 Generally, activation energies for more complex molecules are higher due to the higher number
458 of enzymatic steps needed for biological processing; therefore, per kinetic theory, complex
459 (lower quality) OC should have greater temperature sensitivity than simpler (higher quality) OC
460 (Bosatta and Agren, 1999, Conant et al., 2008, Craine et al., 2010, Conant et al., 2011, Gudasz et
461 al., 2015). This also implies that, as temperatures increase, previously recalcitrant SOM fractions
462 should become bioavailable due to increased ambient thermal energy and increased chemical
463 reaction rates. Temperature data collected from the BH-13 vertical profile at Vault Lake suggest
464 that, as sediments from the F-3 taberite facies historically incubated for centuries *in situ* beneath
465 the lake center, they were exposed to temperatures below 10 ˚C, but not temperatures as high as
466 10 ˚C and 25 ˚C. Over time, our results suggest simpler, higher quality OC compounds may have
467 mineralized *in situ*, leaving behind more complex OC compounds that did not have sufficient
468 activation energies to be processed into CH_4 at the temperatures present in the talik. Remaining
469 fractions of OC may also have been more closely associated with soil minerals, protecting the
470 OC from *in situ* mineralization and increasing potential temperature sensitivities with warming
471 (Gentsch et al., 2018). Increasing temperatures to 10 ˚C and 25 ˚C in the incubations may have
472 provided additional ambient energy to mineralize a fraction of the OC compounds that had not
473 been previously mineralized *in situ*, increasing the potential substrate pool for methanogens. The

474 significant increases in CH_4 production in the F-3 facies at the 10 ˚C and 25 ˚C incubation
475 temperatures (Table 2; Figure 2) supports the suggestion that warming the sediments above *in*
476 *situ* temperatures allowed a greater proportion of SOC to be mineralized. We attempted to run a
477 C pool deconvolution model (Schädel et al., 2014) to estimate the relative sizes of initial SOC
478 quality pools in each of our samples, but were unable to constrain the model parameters because
479 most of our samples did not experience exponential declines in CH_4 production rates during our
480 incubation (Figure S2).
481 Initial microbial communities shifted from predominately methanogens in the F-4 facies
482 to predominately methanotrophs in the F-3 facies. This observed shift in initial microbial
483 communities suggests, in sediments thawed centuries, a significant portion of CH_4 produced *in*
484 *situ* may also be consumed *in situ* (Winkel et al., in review). Even though the initial archaeal
485 community in the F-3 taberite facies showed only anaerobic methanotrophic communities related
486 to *Methanoperedenaceae* at a cut-off of 0.1% relative sequence abundance, we could detect
487 methanogens of mainly *Methanocellales*, *Methanoregulaceae*, *Methanosarcinaceae*, and
488 *Methanosaetaceae* in the rare biosphere (Figure S3), which we defined as taxa below 0.1%
489 relative abundance. We did not detect these rarer taxa of methanogens in the underlying F-4
490 recently thawed taberite or F-5 transitional permafrost facies, suggesting that methanogen
491 communities in the F-3 facies were forced to adapt over time in response to decreasing
492 proportions of available substrate. When we experimentally increased temperatures to 10 ˚C and
493 25 ˚C in our incubations, our results indicate the resultant increase in potential available substrate
494 may have triggered a rapid increase in the abundance of methanogens and subsequent net CH_4
495 production potentials (Knoblauch et al., 2018, Wei et al., 2018). Previous studies have found that
496 optimum temperature ranges for methanogenesis in permafrost soils range from 18 ˚C to 30 ˚C

497 (Tveit et al., 2015, Dean et al., 2018). Thus, experimentally warming sediments from the F-3
498 facies to 25 ˚C may have subsequently increased the availability of potential substrate and
499 triggered a rapid increase in the abundance of methanogens, creating optimal conditions for
500 increases in CH_4 production rates.

501 While CH_4 oxidation rates also increase with increasing temperatures, the temperature
502 responses of anaerobic CH_4 oxidation rates are largely unknown and it has been suggested that
503 CH_4 oxidation rates in sediment are less temperature-dependent than CH_4 production rates
504 (Schipper et al., 2014). Anaerobic incubations of ice wedge polygon cores from Northern Alaska
505 found temperature sensitivity of CH_4 production was 1.7 to 3.7 times higher than the temperature
506 sensitivity of CH_4 oxidation in the same soils (Zheng et al., 2018). The high R values we
507 observed in the F-3 facies at our higher incubation temperatures (10 ˚C and 25 ˚C) compared to
508 our lower temperatures (0 ˚C and 3 ˚C) suggest, in our lake core, warming the thawed permafrost
509 above *in situ* temperatures caused CH_4 production rates to increase more than anaerobic CH_4
510 oxidation rates, leading to increases in net anaerobic CH_4 production potentials. This suggests,
511 with additional warming, active microbial communities in permafrost thawed centuries could
512 potentially shift from predominately methanotrophs to back to predominately methanogens.

513 *4.3. Temperature sensitivities in deposited sediments*

514 Sediments from the F-1 facies, which contained significantly higher levels of recently-
515 deposited SOC, generally produced the most net CH_4 but had the lowest temperature sensitivities
516 in our study. This is consistent with recent findings from aerobic incubations of active layer soils
517 from a different permafrost region, which found that C decomposition rates at 0-10 cm depth
518 were higher than at 20-30 cm depth, but temperature sensitivity of C decomposition was higher
519 in the deeper layer (Li et al., 2018). This is also consistent with prior studies of thermokarst lake

systems, which have shown that the majority (~90%) of CO_2 and CH_4 produced and emitted from Alaskan lakes originates from younger C found in more recently-deposited sediments, as opposed to Pleistocene-aged C found in deeper permafrost (Heslop et al., 2015, Elder et al., 2018). Like the F-4 recently-thawed taberite sediments, which also contained relatively "fresh" SOC from recently-thawed permafrost, the archaeal communities in the F-1 sediments were dominated by methanogens (84% of sequences; Figure 3). This agrees with previous examinations of microbial communities in near-surface thermokarst-lake sediments, which found higher abundance and diversity of methanogens in sediments with higher OM levels (Crevecoeur et al., 2016, Matheus Carnevali et al., 2018). This dominance of methanogens, coupled with high substrate levels and increases in net CH_4 production across all temperature intervals, suggests temperature is a limiting factor in net CH_4 production in this facies and future sediment warming could increase net CH_4 production and emissions from the near-surface lake sediments.

Sediments in the F-2 lacustrine silt facies, which have experienced longer times since deposition (up to 400 years based on estimated lake age; Heslop et al., 2015), had greater temperature sensitivity and higher R values than the more recently-deposited F-1 mud facies. Geochemical data measured by Heslop et al. (2015) show this facies also has lower SOC content than the overlying F-1 facies. We suggest the lower SOC and higher R values in the F-2 facies compared to the F-1 facies are the result of *in situ* CH_4 production over time depleting the most labile substrate. Initial microbial communities in the F-2 lacustrine silt sediments were not analyzed.

Unlike recently-thawed sediments in the taberite chronosequence (F-4, F-5), sediments deposited following lake formation (F-1, F-2) experienced exponential increases in net CH_4 production across all temperature intervals, as indicated by high R^2 values ($R^2 = 0.73$) when

543 fitting the log of CH_4 production versus incubation temperature (Figure 2). Also unlike the
544 thawed taberite chronosequence, we did not observe temperature thresholds where net CH_4
545 production sharply increased in the F-1 and F-2 facies. Differences in *in situ* temperatures may
546 contribute to these differences. Temperature data collected from depth corresponding to the F-1
547 facies in the Vault Lake profiles (0.5 m and 1.0 m depth in both profiles) showed clear seasonal
548 temperature fluctuations at depths consistent with deposited sediments in the F-1 and F-2 facies
549 (Figure 1). In the lake center (BH13), shallow sediments experienced *in situ* seasonal
550 temperature variations ranging from 1.26 ˚C to 4.51 ˚C; sediments in the near-shore profile
551 (BH10) experienced larger seasonal fluctuations of 0.14 ˚C to 14.45 ˚C. This suggests microbial
552 communities in deposited sediments seasonally adapt in response to fluctuating temperatures,
553 and thus may have been more readily responsive to warming during our incubations.

554 *4.4. Conclusions*

555 In this study, we used microbiological data and trends in net CH_4 production potentials to
556 show that century-scale time since permafrost thaw affects both methanogen community
557 composition and temperature sensitivity of CH_4 production. We suggest that these changes are
558 due to changes in SOC quality and *in situ* microbial community composition over time. While
559 we only examined one core and further research is necessary to determine if our findings are
560 widespread across different thermokarst lake environments, our approach of using sediments
561 from a core collected from a thermokarst lake talik is particularly relevant in refining estimates
562 of the long-term magnitude and timing of the PCF given that, with climate warming, taliks are
563 anticipated to become widespread in northern permafrost regions, covering up to 14 million km^2
564 and emitting up to 120 Pg C by 2300 (Parazoo et al., 2018).

Recently-thawed sediments (decadal time scales since thaw) collected from the F-4 recently-thawed taberite and F-5 transitional permafrost were most sensitive to warming at lower temperatures. Initial microbial community composition data suggest the increases in net CH_4 production are due to the establishment of stable, cold-adapted CH_4-producing communities in the years to decades following thaw. Increased time since thaw (century time scales) in the F-3 taberite lead to a shift in initial microbial communities from being predominately methanogens (F-4) to predominately methanotrophs (F-3). However, in the F-3 facies we also observed the highest overall CH_4 production temperature sensitivities and significant increases in net CH_4 production when we experimentally increased temperatures above observed *in situ* temperatures, suggesting additional ambient energy allows a greater proportion of thawed OC to be mineralized and microbes associated with CH_4 production had a greater temperature response than microbes associated with CH_4 oxidation. This suggests, on centuries time scales following permafrost thaw, additional warming could potentially reduce mitigation effects of CH_4 oxidation. In contrast to the thawed permafrost sequence (F-3, F-4, F-5), sediments deposited following lake formation (F-1 and F-2) generally followed exponential increases in CH_4 production across the full incubation temperature range and had the lowest overall temperature sensitivity values. This suggests our observed thresholds where net CH_4 production sharply increased in the thawed permafrost sequence (F-3, F-4, F-5) are a property of time since permafrost thaw.

Acknowledgements

We thank P. Anthony, S. Billings, A. Bondurant, J. Cherry, M. Engram, N. Haubenstock, F. Horn, T. Howe, K. Martinez-Cruz, P. Lindgren, A. Saborowski, C. Schädel, A. Sepulveda-

588 Jauregui, and M. Zhang for assistance in data collection and/or analysis; C. Knoblauch, V.
589 Romanovsky, M. Zhang, and three anonymous reviewers for their feedback on earlier versions of
590 this manuscript; and S. Skidmore for granting access to Vault Lake. Funding for J.K.H. and
591 K.M.W.A. was provided NSF ARC-1304823 and ARC-1500931 and NASA ABoVE
592 NNX15AU49A. M. W. was supported by the NSF ARCSS-1500931. G.G. was additionally
593 supported by ERC 338335. The Helmholtz Gemeinschaft (HGF) is acknowledged for funding
594 the Young Researcher's Group of S.L. (VH-NG-919). Additional funding for J.K.H. was
595 provided under STAR Fellowship Assistance agreement no. FP-91762901-0 awarded by the US
596 Environmental Protection Agency (EPA). The publication has not been formally reviewed by the
597 EPA. The views expressed in this publication are solely those of the authors and the EPA does
598 not endorse any products or commercial services mentioned.

Tables

Table 1. Initial characteristics of each sediment subsample (n = 1 subsample per depth), modified from Heslop et al. (2015).

Sample ID	Facies	Depth in Core (cm)	Geochemistry SOC (% wt)	N (% wt)	SOC:N
F-1	Surface organic-rich mud	8	4.8*	0.5*	10.6
F-2	Lacustrine silt	178	1.6	0.1	17.8
F-3	Taberite	384	1.0	0.1	9.6
F-4	Recently-thawed taberite	550	1.1	0.1	9.2
F-5	Frozen transitional permafrost	582	1.1	0.2	6.6

* Statistically significant ($p \leq 0.05$) difference from other facies

603 **Table 2.** Ratios of cumulative net C-CH_4 production potentials between incubation temperatures.
604 Ratios were calculated using mean cumulative net C-CH_4 production potentials from the
605 triplicate incubation vials.

Facies	3 ºC : 0 ºC	10 ºC : 0 ºC	25 ºC : 0 ºC	10 ºC : 3 ºC	10 ºC : 3 ºC	25 ºC : 10 ºC
F-1	1.1	9.9	14.0 $^{\gamma}$	8.6	12.2	1.4 $^{\gamma}$
F-2	4.1	131 $^{\gamma}$	436 $^{\gamma}$	32.4 $^{\gamma}$	107 $^{\gamma}$	3.3 $^{\gamma}$
F-3	5.1	1,470 $^{\gamma}$	99,200 $^{\gamma}$	289 $^{\gamma}$	19,400 $^{\gamma}$	67.3 $^{\gamma}$
F-4	365	4.7 $^{\gamma}$	86.5 $^{\gamma}$	0.01 $^{\gamma}$	0.24 $^{\gamma}$	18.4 $^{\gamma}$
F-5	46.4	140 $^{\gamma}$	20.9 $^{\gamma}$	3.0 $^{\gamma}$	0.45 $^{\gamma}$	0.15 $^{\gamma}$

$^{\gamma}$ Higher incubation temperature warmer than *in situ* temperatures observed at similar depth in the Vault Lake talik (Fig. 1)

606

Figures

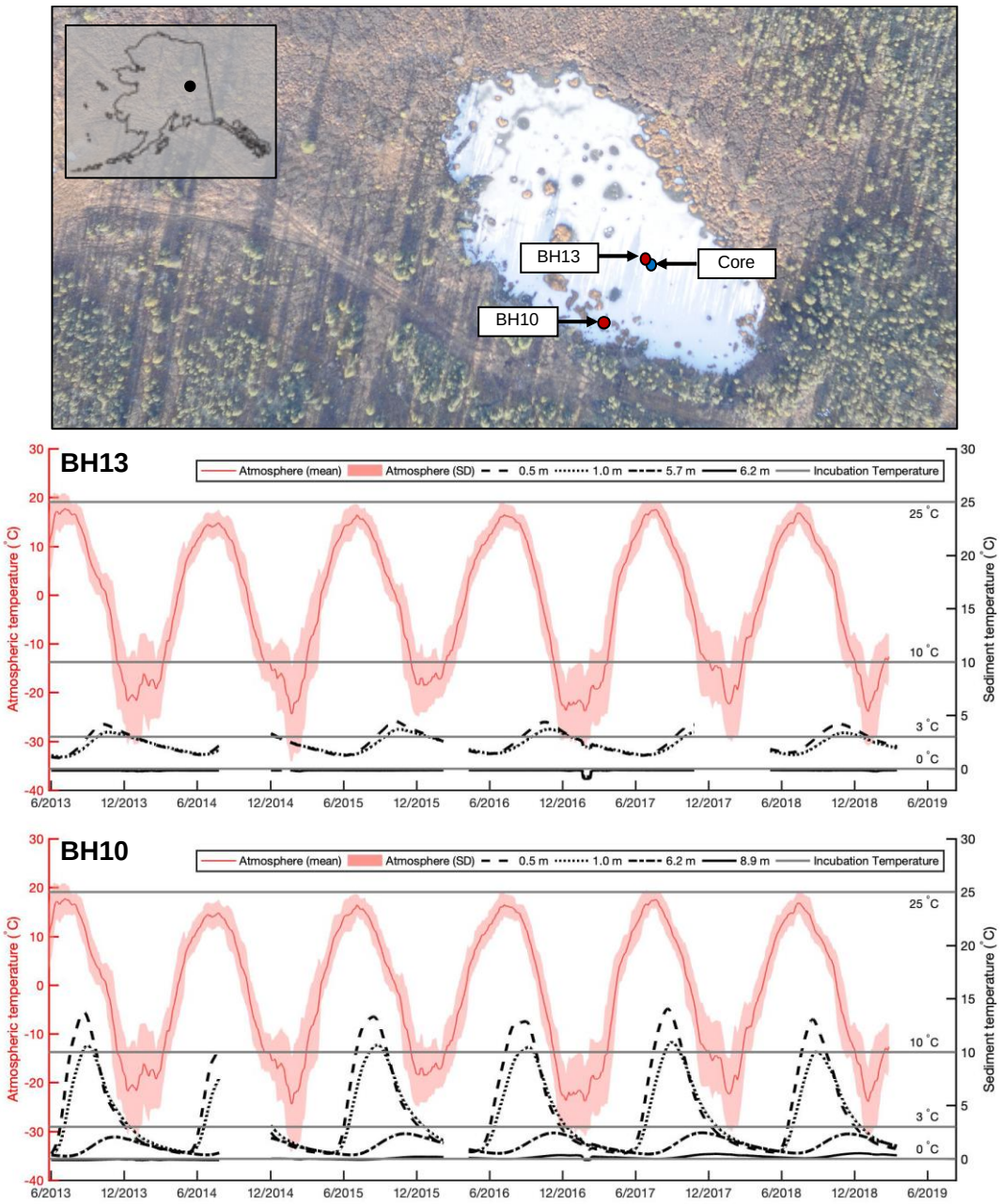

Figure 1. Location map of Vault Lake and the sediment core and temperature profile locations within Vault Lake. The aerial photograph of Vault Lake was taken 14 October 2011 by J. Cherry. Temperature data at Vault Lake were recorded hourly from May 2013 through April 2019 at BH13 and BH10. Temperature sensor depths are representative of the F-1 surface organic-rich mud (BH10 and BH13: 0.5 m and 1.0 m), the F-3 taberite (BH10: 6.2 m), the F-4 recently-thawed taberite (BH13: 5.7 m), and the F-5 frozen transitional permafrost (BH10: 8.9 m, BH13: 6.2 m) facies. Atmospheric temperature data are mean ± SD daily mean temperatures from Fairbanks, AK (ACIS Station Fairbanks AP #2) during the same time period.

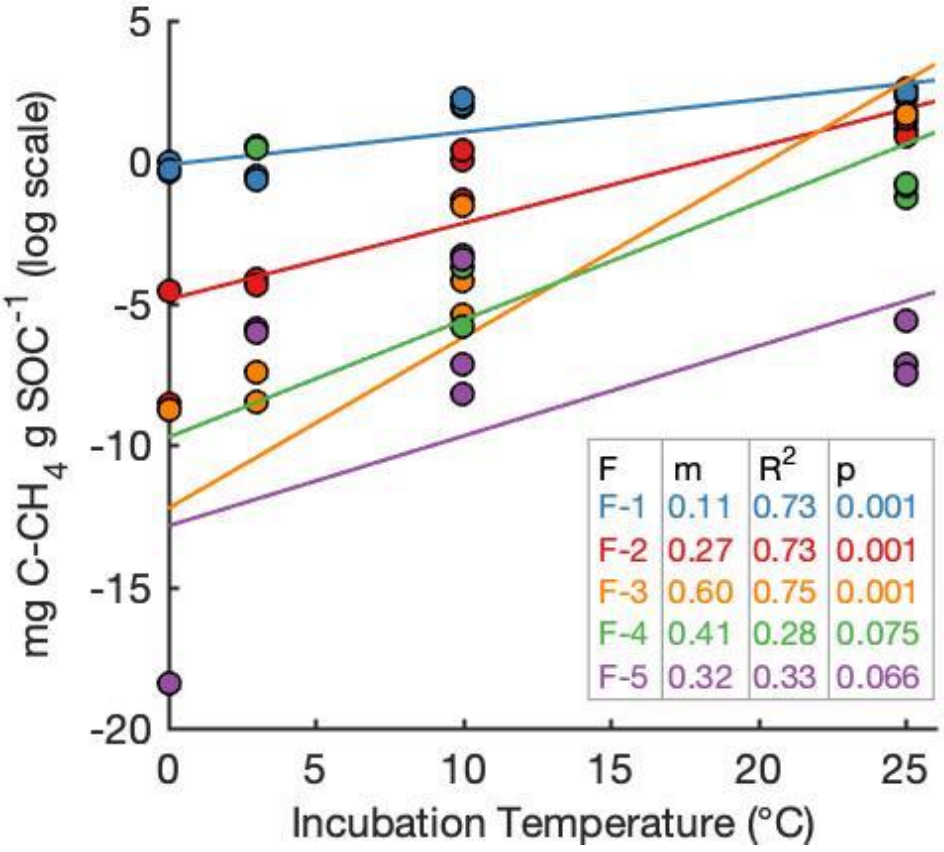

Figure 2. Net methane (C-CH_4) production potentials and temperature sensitivities during the 150-day anaerobic incubation period at four incubation temperatures. Analytical error bars for CH_4 production are not visible due to error being smaller than the marker size. Temperature sensitivities were calculated using linear regression as the slope of net C-CH_4 production potentials versus the incubation temperature; each point represents one incubation vial (n = 12 observations per facies). Please see Table S1 in the supplementary information for 95% confidence intervals of calculated temperature sensitivity slope parameters.

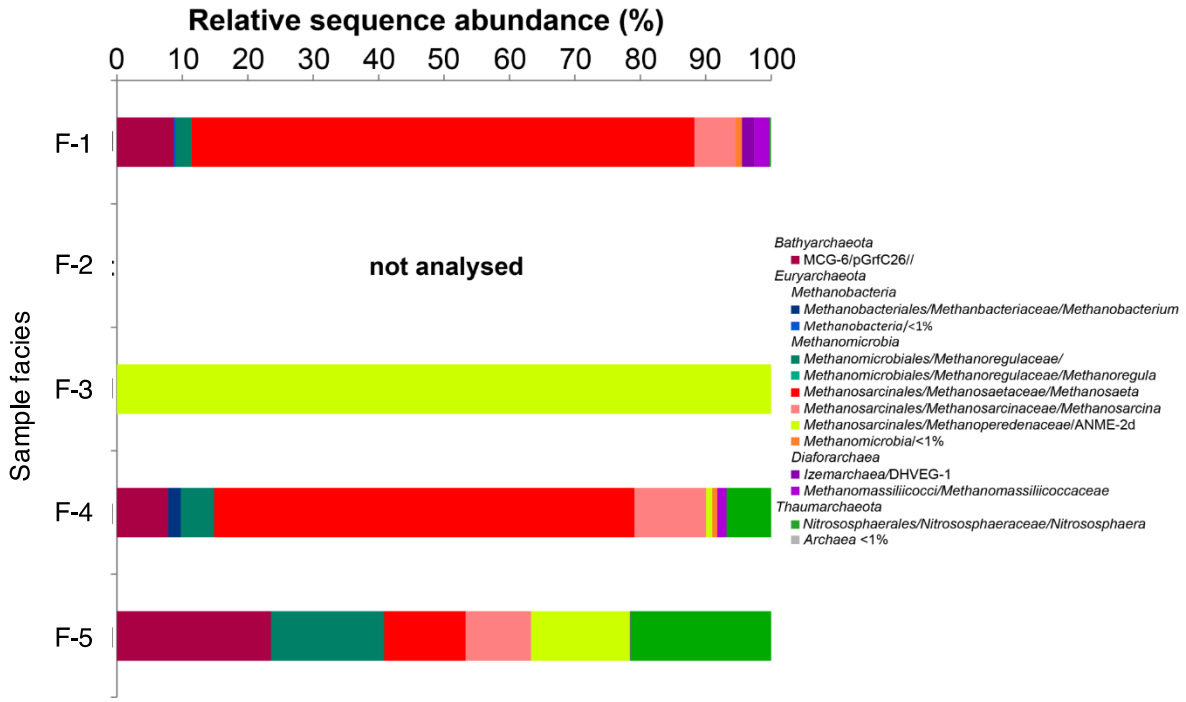

Figure 3. Relative sequence abundance of archaeal 16S rRNA genes in sediment facies of the Vault lake core. Archaeal taxa over 0.1% relative abundance are shown to genus level.

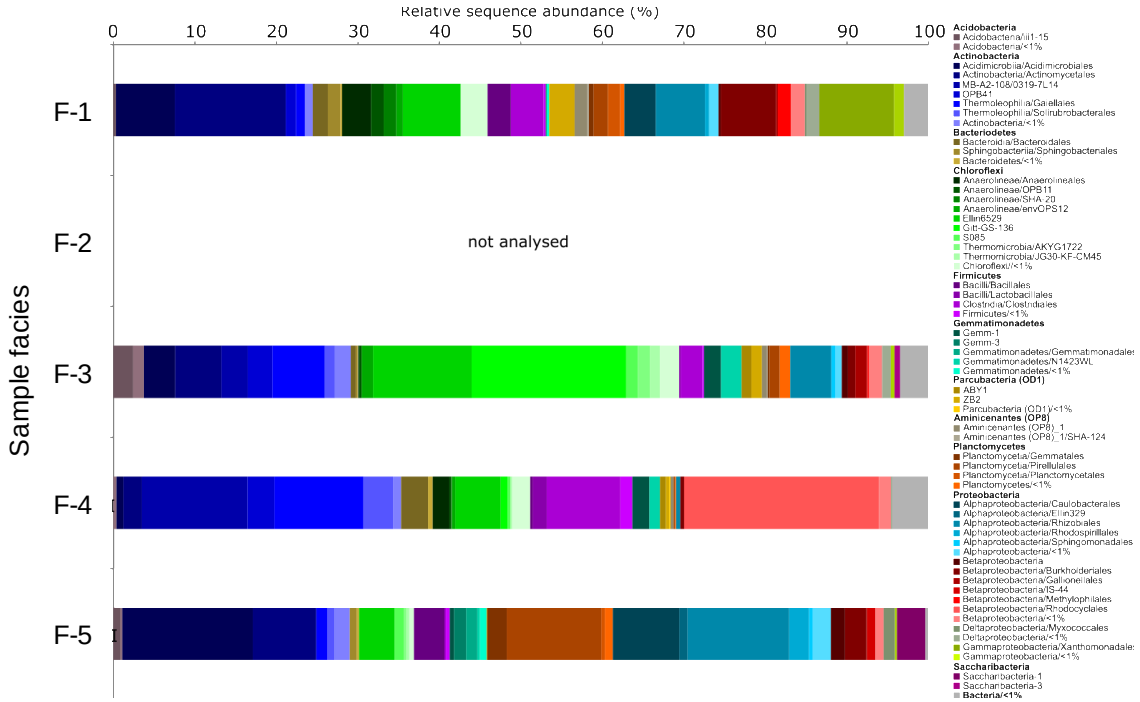

Figure 4. Relative sequence abundance of bacterial 16S rRNA genes in sediment facies of the Vault lake core. Bacterial taxa over 0.1% relative abundance are shown to order level.

References

Adam, P.S., Borrel, G., Brochier-Armanet, C., Gribaldo, S., 2017. The growing tree of Archaea: new perspectives on their diversity, evolution and ecology. ISME J. 11, 2407-2425. doi:10.1038/ismej.2017.122.

Bekryaev, R., Polyakov, I., Alexeev, V., 2010. Role of Polar Amplification in Long-Term Surface Air Temperature Variations and Modern Arctic Warming. Journal of Climate, 23, 3888–3906.

Biskaborn, B.K., Smith, S.L., et al., 2019. Permafrost is warming at a global scale. Nature Communications, 10, 264. doi: 10.1038/s41467-018-08240-4

Bolger, A.M., Lohse, M., Usadel, B., 2014. Trimmomatic: a flexible trimmer for Illumina sequence data. Bioinformatics, 30, 2114–2120.

Bracho, R., Natali, S., Pegoraro, E., et al., 2016. Temperature sensitivity of organic matter decomposition of permafrost-region soils during laboratory incubations. Soil Biology and Biochemistry, 97, 1-14.

Brosius, L., Walter Anthony, K.M., Grosse, G., et al., 2012. Using the deuterium isotope composition of permafrost meltwater to constrain thermokarst lake contributions to atmospheric CH_4 during the last deglaciation. Journal of Geophysical Research Biogeosciences 117, G01022.

Čapek, P., Diáková, K., Dickopp, J.-E., et al., 2015. The effect of warming on the vulnerability of subducted organic carbon in arctic soils. Soil Biology and Biochemistry, 90, 19–29.

Caporaso, J.G., Kuczynski, J., Stombaugh, J., Bittinger, K., Bushman, F.D., Costello, E.K., et al., 2010. QIIME allows analysis of high-throughput community sequencing data. Nat Methods, 7, 335–336.

Castelle, C.J., Wrighton, K.C., Thomas, B.C., Hug, L.A., Brown, C.T., Wilkins, M.J., et al., 2015. Genomic Expansion of Domain Archaea Highlights Roles for Organisms from New Phyla in Anaerobic Carbon Cycling. Curr Biol, 25, 690–701.

Chowdhury, R.T., Herndon, E.M., Phelps, T.J., 2015. Stoichiometry and temperature sensitivity of methanogenesis and CO_2 production from saturated polygonal tundra in Barrow, Alaska. Global Change Biology, 21, 722-737.

Conant, R.T., Drijber, R.A., Haddix, M.L., 2008. Sensitivity of organic matter decomposition to warming varies with its quality. Global Change Biology, 14, 868-877.

Conant, R.T., Ryan, M.G., Ågren, G.I., et al., 2011. Temperature and soil organic matter decomposition rates- synthesis of current knowledge and a way forward. Global Change Biology, 17, 3392–3404.

Craine, J., Fierer, N., McLauchlan, K., 2010. Widespread coupling between the rate and temperature sensitivity of organic matter decay. Nature Geoscience, 3, 854–857.

Crevecoeur, S., Vincent, W.F., and Lovejoy, C., 2016. Environmental selection of planktonic methanogens in permafrost thaw ponds. Scientific Reports, 6, 31312. doi: 10.1038/srep31312

Davidson, E.A., Janssens, I.A., 2006. Temperature sensitivity of soil carbon decomposition and feedbacks to climate change. Nature, 440, 165-173.

Dean, J., Middelburg, J., Röckmann, T., et al., 2018. Methane feedbacks to the global climate system in a warmer world. Reviews of Geophysics, 56, 207-250.

de Jong, A.E.E., in ‘t Zandt, M.H., Meisel, O.H., et al., 2018. Increases in temperature and nutrient availability positively affect methane-cycling microorganisms in Arctic thermokarst lake sediments. Environmental Microbiology, 20(12): 4314-4327.

680 Drake, T., Wickland, K., Spencer, R., McKnight, D., Striegl, R., 2015. Ancient low–molecular-
681 weight organic acids in permafrost fuel rapid carbon dioxide production upon thaw.
682 Proceedings of the National Academy of Sciences, 112, 13946–13951.
683 Elder, C., Xu, X., Walker, J., Schnell, J., et al., 2018. Greenhouse gas emissions from diverse
684 Arctic Alaskan lakes are dominated by young carbon. Nature Climate Change, 8(2), 166-
685 171.
686 Ewing, S., O'Donnell, J., Aiken, G., Butler, K., Butman, D., Windham-Myers, L., Kanevskiy,
687 M., 2015. Long-term anoxia and release of ancient, labile carbon upon thaw of
688 Pleistocene permafrost. Geophysical Research Letters, 42, 10,730–10,738.
689 Fey, A., Conrad, R., 2000. Effect of Temperature on Carbon and Electron Flow and on the
690 Archaeal Community in Methanogenic Rice Field Soil. Applied and Environmental
691 Microbiology, 66, 4790–4797.
692 Gentsch, N., Wild, B., Mikutta, R., et al., 2018. Temperature response of permafrost soil carbon
693 is attenuated by mineral protection. Global Change Biology 24, 8, 3401-3415. doi:
694 10.1111/gcb.14316
695 Glassman, S.I., Weihe, C., Li, J., et al., 2018. Decomposition responses to climate depend on
696 microbial community composition. PNAS. doi: 10.1073/pnas.1811269115.
697 Graham, D., Wallenstein, M., Vishnivetskaya, T., et al., 2012. Microbes in thawing permafrost:
698 the unknown variable in the climate change equation. The ISME Journal, 6, 709–712.
699 Grosse, G., Jones, B., Arp, C., 2012. Thermokarst Lakes, Drainage, and Drained Basins, in:
700 Treatise on Geomorphology, edited by: Shroder, J. F., Academic Press, San Diego, 325-
701 353.

Gudasz, C., Sobek, S., Bastviken, D., 2015. Temperature sensitivity of organic carbon mineralization in contrasting lake sediments. Journal of Geophysical Research: Biogeosciences, 120, 1215–1225.

Guo, D., Wang, H., 2016. CMIP5 permafrost degradation projection: A comparison among different regions. Journal of Geophysical Research: Atmospheres, 121, 4499–4517.

He, R., Wooller, M.J., Pohlman, J.W., et al. Diversity of active anaerobic methanotrophs along depth profiles of arctic and subarctic lake water column and sediments. The ISME Journal, 6, 1937-1948.

Herlemann, D.P., Labrenz, M., Jürgens, K., Bertilsson, S., Waniek, J.J., Andersson, A.F., 2011. Transitions in bacterial communities along the 2000 km salinity gradient of the Baltic Sea. ISME J, 5, 1571–1579.

Heslop, J.K., Walter Anthony, K.M., Sepulveda-Jauregui, A., Martinez-Cruz, K., Bondurant, A., Grosse, G., Jones, M.C., 2015. Thermokarst lake methanogenesis along a complete talik profile. Biogeosciences, 12, 4317–4331.

Heslop, J.K., Walter Anthony, K.M., Zhang, M., 2017. Utilizing pyrolysis GC-MS to characterize organic matter quality in relation to methane production in a thermokarst lake sediment core. Organic Geochemistry, 103, 43-50.

Heslop, J.K., Winkel, M.,Walter Anthony, K.M., Spencer, R.G.M., Podgorski, D.C., Zito, P., Kholodov, A., Zhang, M., Liebner, S., 2019. Increasing organic carbon biolability with depth in yedoma permafrost: ramifications for future climate change. Journal of Geophysical Research: Biogeosciences, doi: 10.1029/2018JG004712.

723 Hugelius, G., Strauss, J., Zubrzycki, S., et al., 2014. Estimated stocks of circumpolar permafrost
724 carbon with quantified uncertainty ranges and identified data gaps. Biogeosciences, 11,
725 6573–6593.
726 Jorgenson, T., Harden, J., Kanevskiy, M., et al., 2013. Reorganization of vegetation, hydrology
727 and soil carbon after permafrost degradation across heterogeneous boreal landscapes.
728 Environmental Research Letters, 8, 035017.
729 Kessler, M.A., Plug, L.J., Walter Anthony, K.M., 2012. Simulating the decadal- to millennial-
730 scale dynamics of morphology and sequestered carbon mobilization of two thermokarst
731 lakes in NW Alaska. Journal of Geophysical Research: Biogeosciences, 117, G00M06.
732 Kling, G., Kipphut, G., 1991. Arctic lakes and streams as gas conduits to the atmosphere:
733 implications for tundra carbon budgets. Science, 251, 298-301.
734 Knoblauch, C., Beer, C., Sosnin, A., Wagner, D., Pfeiffer, E.-M., 2013. Predicting long-term
735 carbon mineralization and trace gas production from thawing permafrost of Northeast
736 Siberia. Global Change Biology, 19, 1160–1172.
737 Knoblauch, C., Beer, C., Liebner, S., Grigoriev, M.N., Pfeiffer, E.-M., 2018. Methane production
738 as key to the greenhouse gas budget of thawing permafrost. Nature Climate Change, doi:
739 10.1038/s41558-018-0095-z
740 Lenz, J., Jones, B., Wetterich, S., et al., 2016. Impacts of shore expansion and catchment
741 characteristics on lacustrine thermokarst records in permafrost lowlands, Alaska Arctic
742 Coastal Plain. Arktos, 2:25.
743 Li, J., Yan, D., Pendall, E., et al., 2018. Depth dependence of soil carbon temperature sensitivity
744 across Tibetan permafrost regions. Soil Biology and Biochemistry, 126:82-90. doi:
745 10.1016/j.soilbio.2018.08.015

746 Mackelprang, R. et al. (2017), Microbial survival strategies in ancient permafrost: insights from
747 metagenomics, The ISME Journal, 1-14, doi:10.1038/ismej.2017.93.
748 Malard, L., and D. Pearce (2018), Microbial diversity and biogeography in Arctic soils, Env
749 Microbiol Rep, doi:10.1111/1758-2229.12680.
750 Matheus Carnevali, P.B., Herbold, C.W., Hand, K.P., et al., 2018. Distinct microbial assemblage
751 structure and archaeal diversity in sediments of Arctic thermokarst lakes differing in
752 methane sources. Front. Microbiol., doi: 10.3389/fmicb.2018.01192.
753 Martin, M., 2011. Cutadapt removes adapter sequences from high-throughput sequencing reads.
754 EMBnet.journal, 17, 10–12.
755 Michaelson, G.J., Ping, C.L., 2003. Soil organic carbon and CO_2 respiration at subzero
756 temperature in soils of Arctic Alaska. Journal of Geophysical Research, 108, 8164.
757 Mikan, C.J., Schimel, J.P., Doyle, A.P., 2002. Temperature controls of microbial respiration in
758 arctic tundra soils above and below freezing. Soil Biology and Biochemistry, 34, 1785-
759 1795.
760 Myhre, G., Shindell, D., Breon, F.M., et al., 2013. Anthropogenic and Natural Radiative Forcing.
761 In: Climate Change 2013: The Physical Science Basis. Contribution of Working Group I
762 to the Fifth Assessment Report of the Intergovernmental Panel on Climate Change.
763 Intergovernmental Panel on Climate Change, New York, USA.
764 Negandhi, K., Laurion, I., Whiticar, M.J., et al., 2013. Small thaw ponds: an unaccounted source
765 of methane in the Canadian High Arctic. PLOS ONE, doi: 10.1371/journal.pone.0078204
766 Olefeldt, D., Turetsky, M., Crill, P., McGuire, D., 2013. Environmental and physical controls on
767 northern terrestrial methane emissions across permafrost zones. Global Change Biology,
768 19, 589–603.

769 Parazoo, N. C., Koven, C. D., Lawrence, D. M., Romanovsky, V., and Miller, C. E.: Detecting
770 the permafrost carbon feedback: talik formation and increased cold-season respiration as
771 precursors to sink-to-source transitions, The Cryosphere, 12, 123-144,
772 https://doi.org/10.5194/tc-12-123-2018, 2018.
773 Plug, L., West, J., 2008. Thaw lake expansion in a two-dimensional coupled model of heat
774 transfer, thaw subsidence, and mass movement. Journal of Geophysical Research, 114,
775 F01002.
776 Quast, C., Pruesse, E., Yilmaz, P., Gerken, J., Schweer, T., Yarza, P., et al., 2012. The SILVA
777 ribosomal RNA gene database project: improved data processing and web-based tools.
778 Nucleic Acids Res, 41, D590–D596.
779 Rinke, C., Schwientek, P., Sczyrba, A., Ivanova, N.N., Anderson, I.J., Cheng, J.-F., et al., 2013.
780 Insights into the phylogeny and coding potential of microbial dark matter. Nature, 499,
781 431–437.
782 Schädel, C., Schuur, E., Bracho, R., et al., 2014. Circumpolar assessment of permafrost C quality
783 and its vulnerability over time using long-term incubation data. Global Change Biology,
784 20, 641–652.
785 Schädel, C., Bader, M., Schuur, E., et al., 2016. Potential carbon emissions dominated by carbon
786 dioxide from thawed permafrost soils. Nature Climate Change, 6, 950-953.
787 Schipper, L., Hobbs, J., Rutledge, S., Arcus, V., 2014. Thermodynamic theory explains the
788 temperature optima of soil microbial processes and high Q_{10} values at low temperatures.
789 Global Change Biology, 20, 3578–86.
790 Schuur, E., McGuire, A., Schädel, C., et al., 2015. Climate change and the permafrost carbon
791 feedback. Nature, 520, 171–179.

792 Sepulveda-Jauregui, A., Walter Anthony, K.M., Martinez-Cruz, K., Greene, S., Thalasso, F.,
793 2015. Methane and carbon dioxide emissions from 40 lakes along a north south
794 latitudinal transect in Alaska. Biogeosciences, 12, 3197–3223.
795 Spencer. R., Mann, P., Dittmar, T., et al., 2015. Detecting the signature of permafrost thaw in
796 Arctic rivers. Geophysical Research Letters, 42, 2830–2835.
797 Strauss, J. et al., 2017. Deep Yedoma permafrost: A synthesis of depositional characteristics and
798 carbon vulnerability. Earth-sci Rev, 172, 75–86, doi:10.1016/j.earscirev.2017.07.007.
799 Treat, C.C., Natali, S.M., Ernakovich, J., et al., 2015. A pan-Arctic synthesis of CH_4 and CO_2
800 production from anoxic soil incubations. Global Change Biology, 21, 2787–2803.
801 Tveit, A.T., Urich, T., Frenzel, P., Svenning, M.M., 2015. Metabolic and trophic interactions
802 modulate methane production by Arctic peat microbiota in response to warming. Proc
803 Natl Acad Sci, 201420797.
804 Vonk, J.E., Tank, S.E., Mann, P.J., Spencer, R.G.M., Treat, C.C., Striegl, R.G., Abbott, B.W.,
805 Wickland. K.R., 2015. Biodegradability of dissolved organic carbon in permafrost soils
806 and aquatic systems: a meta-analysis. Biogeosciences, 12, 6915–30.
807 Walter, K., Zimov, S., Chanton, J., Verbyla, D., Chapin, F., 2006. Methane bubbling from
808 Siberian thaw lakes as a positive feedback to climate warming. Nature, 443, 71–75.
809 Walter, K., Edwards, M., Grosse, G., Zimov, S., Chapin, F., 2007. Thermokarst Lakes as a
810 Source of Atmospheric CH_4 During the Last Deglaciation. Science, 318, 633–636.
811 Walter, K., Chanton, J., Chapin, F., Schuur, E., Zimov, S., 2008. Methane production and bubble
812 emissions from arctic lakes: Isotopic implications for source pathways and ages. Journal
813 of Geophysical Research: Biogeosciences (2005–2012), 113.

814 Walter Anthony, K.M., Anthony, P., 2013. Constraining spatial variability of methane ebullition
815 seeps in thermokarst lakes using point process models. Journal of Geophysical Research:
816 Biogeosciences,118, 1015–1034.
817 Walter Anthony, K.M., Zimov, S.A., Grosse, G., et al., 2014. A shift of thermokarst lakes from
818 carbon sources to sinks during the Holocene epoch. Nature, 511, 452–456.
819 Walter Anthony, K.M., et al., 2018. 21st-century modeled permafrost carbon emissions
820 accelerated by abrupt thaw beneath lakes. Nature Communications, 9, 3262.
821 Wagner, D., Gattinger, A., Eacher, A., Pfeiffer, E., Schloter, M., Lipski, A., 2007. Methanogenic
822 activity and biomass in Holocene permafrost deposits of the Lena Delta, Siberian Arctic
823 and its implication for the global methane budget. Global Change Biology, 13, 1089–
824 1099.
825 Wen, X., Yang, S., Horn, F., Winkel, M., Wagner, D., Liebner, S., 2017. Global biogeographic
826 analysis of methanogenic archaea identifies community-shaping environmental factors of
827 natural environments. Front. Microbiol. 8. doi:10.3389/fmicb.2017.01339.
828 Winkel, M., Sepulveda-Jauregui, A., et al., 2019. First evidence for cold-adapted anaerobic
829 oxidation of methane in deep sediments of thermokarst lakes. Environmental Research
830 Communications, 1, 021002.
831 Yang, Z., Wullschleger, S., Liang, L., Graham, D., Gu, B., 2016. Effects of warming on the
832 degradation and production of low-molecular-weight labile organic carbon in an Arctic
833 tundra soil. Soil Biology and Biochemistry, 95, 202–211.
834 Yvon-Durocher, G., Caffrey, J., Cescatti, A., et al., 2012. Reconciling the temperature
835 dependence of respiration across timescales and ecosystem types. Nature, 487, 472–476.

836 Zhang, J., Kobert, K., Flouri, T., Stamatakis, A., 2014. PEAR: a fast and accurate Illumina
837 Paired-End reAd mergeR. Bioinformatics, 30, 614–620.
838 Zheng, J., Roy-Chowdhury, T., Yang, Z., et al., 2018. Impacts of temperature and soil
839 characterisitcs on methane production and oxidation in Arctic tundra. Biogeosciences, 15,
840 6621-6635. doi: 10.5194/bg-15-6621-2018
841 Zhou, J., Bruns, M.A., Tiedje, J.M., 1996. DNA recovery from soils of diverse composition.
842 Appl Environ Microbiol, 62, 316–322.
843 Zimov, S.A., et al., 1997. North Siberian lakes: A methane source fueled by Pleistocene carbon.
844 Science, 277, 800-802.
845 Zimov, S., et al., 2006. Permafrost carbon: Stock and decomposability of a globally significant
846 carbon pool. Geophysical Research Letters, 33(20), doi:10.1029/2006GL027484.